

# Dynamics of Disordered Diblocks of Polyisoprene and Polyvinylethylene

B. H. Arendt, R. Krishnamoorti,<sup>†</sup> R. M. Kannan,<sup>‡</sup> K. Seitz, and J. A. Kornfield\*

Division of Chemistry and Chemical Engineering, California Institute of Technology, Pasadena, California 91125, Department of Chemical Engineering, University of Houston, Houston, Texas 77204, and 3M Center, St. Paul, Minnesota 55144

J. Roovers

Institute for Environmental Chemistry, National Research Council of Canada, Ottawa, Ontario, CANADA K1A 0R6

Received June 21, 1996; Revised Manuscript Received December 3, 1996<sup>®</sup>

**ABSTRACT:** The apparent thermorheological simplicity of disordered diblocks is reconciled with the failure of time–temperature superposition of corresponding miscible blends by examining the relaxation of the constituent blocks using rheo-optical techniques. Diblocks of 1,4-polyisoprene (PIP) and polyvinylethylene (PVE) are examined over a range of temperatures for two compositions ( $\phi_{\text{PIP}} = 0.25$  and 0.75). Unlike blends of PIP and PVE, the block copolymers appear to obey time–temperature superposition on the basis of their viscoelastic properties. However, departure from thermorheological simplicity is exposed in their stress–optical behavior. In particular, the copolymer rich in the high  $T_g$  component ( $\phi_{\text{PIP}} = 0.25$ ) shows distinct temperature dependencies for the individual blocks, in accord with the behavior of PIP/PVE blends. The block copolymer rich in the low  $T_g$  component ( $\phi_{\text{PIP}} = 0.75$ ) is thermorheologically simple because both blocks have similar monomeric friction coefficients  $\zeta_{0,\text{PVE}} \approx \zeta_{0,\text{PIP}}$ , again in accord with prior results on PIP/PVE blends. The failure of time–temperature superposition in these diblocks was not previously observed because the change in  $\zeta_{0,\text{PVE}}/\zeta_{0,\text{PIP}}$  with temperature produces subtle changes in the overall relaxation spectrum relative to a linear chain of uniform friction.

## 1. Introduction

Toward the goal of predicting the processing behavior of blends, it is necessary to understand the effects of composition and temperature on the dynamics of distinct homopolymers and block copolymers. Just as miscible blends provide model systems for investigating the dynamics of each species in a given mixed phase,<sup>1,2</sup> disordered block copolymers represent model systems for probing the dynamics of block copolymers dissolved in a given phase in a blend. The viscoelastic properties of disordered diblock copolymers far from the ordering transition are similar to linear homopolymers. Departures from time–temperature superposition have been reported in the disordered state as the ordering transition is approached, attributed to the development of large composition fluctuations that relax on a longer time scale than the individual chains.<sup>3</sup> However, an additional source of thermorheological complexity is expected due to the distinct temperature dependence of the segmental mobility of each block. In miscible blends this effect is readily apparent in the failure of time–temperature superposition.<sup>4</sup> To unambiguously examine the corresponding effect in block copolymers, it is necessary to suppress the tendency to segregate by using systems in which  $\chi < 0$ . Block copolymers of PIP and PVE<sup>5–8</sup> provide a particularly attractive model system since  $\chi$  is slightly negative and the segmental dynamics of the constituent polymers as functions of composition and temperature have been extensively studied.<sup>1,2,4,9–13</sup>

In bidisperse blends of 1,4-polyisoprene (PIP) and polyvinylethylene (PVE), time–temperature superposition has been shown to fail dramatically.<sup>4,9</sup> Their thermorheological complexity reflects the distinct temperature dependences of the relaxation of each component, described by monomeric friction coefficients  $\zeta_{0,\text{PIP}}(\phi, T)$  and  $\zeta_{0,\text{PVE}}(\phi, T)$ . These two friction coefficients depend differently on both blend composition,  $\phi$  (weight fraction of PIP), and temperature,  $T$ .<sup>1,2,4</sup> For blends rich in PVE the values of  $\zeta_{0,\text{PIP}}(\phi, T)$  and  $\zeta_{0,\text{PVE}}(\phi, T)$  are most disparate, and it is in these blends that the largest departures from thermorheological simplicity are observed.

Paradoxically, rheological studies of diblock copolymers of PIP–PVE show no such failure of time–temperature superposition.<sup>6</sup> This apparent loss of dynamic heterogeneity in miscible block copolymers relative to blends is not evident in local segmental motions that control the glass transition. The DSC traces of the diblock copolymers and blends of the same overall composition are similar, implying similar distributions of local segmental mobilities in the block copolymer and blend.<sup>5–7</sup> More selective probes of segmental mobility also show that each component (PIP or PVE) has similar local dynamics whether in blends or diblocks of a given PIP:PVE ratio.<sup>8,13</sup> To determine why dynamic heterogeneity of miscible blends and corresponding diblocks are similar on a local scale, but qualitatively different on a larger scale, requires further information on conformational relaxation of the diblocks. Rheo-optical methods that can extract the dynamics of each species, even for completely overlapping relaxations are well suited to observe the relative relaxations of each block of the block copolymers.

Previous observations on PIP/PVE blends suggest an explanation for the lack of obvious dynamic heterogeneity in the conformational relaxation of PIP–PVE block

\* Correspondence to: Professor Julia A. Kornfield, Chemical Engineering 210-41, California Institute of Technology, Pasadena, CA 91125.

<sup>†</sup> University of Houston.

<sup>‡</sup> 3M Center.

<sup>®</sup> Abstract published in *Advance ACS Abstracts*, February 1, 1997.

**Table 1. Polyisoprene–Polyvinylethylene Diblock Copolymers from J. Roovers**

| sample                      | 75–25 PIP–PVE,<br>$\phi_{\text{PIP}} = 0.76$ | 25–75 PIP–PVE,<br>$\phi_{\text{PIP}} = 0.25$ |
|-----------------------------|--|--|
| $M_w$ (kg/mol) <sup>a</sup> | 366  | 242  |
| $M_w/M_n$ <sup>a</sup>      | 1.08   | 1.06   |
| $N_{e,\text{PIP}}$          | 49   | 11   |
| $N_{e,\text{PVE}}$          | 24   | 49   |
| % vinyl (PVE) <sup>a</sup>  | 94   | 98   |
| $T_g$ (°C) <sup>a</sup>     | -57  | -25  |

<sup>a</sup> From Roovers and Wang, *J. Non-Cryst. Solids* **1994**, 172–4, 698.

copolymers (BCPs). In blends of PIP and PVE with molecular weights chosen so that the two components have comparable terminal relaxation times in the blend, i.e., both species are approximately equally entangled, the failure of time–temperature superposition is subtle.<sup>1,15,16</sup> When the relaxation spectrum resembles that of a monodisperse polymer, the modest difference between the temperature dependencies of the component friction coefficients leads to small changes in the shape of the frequency dependence of the dynamic moduli with temperature. Thus, on the basis of the results for equally entangled blends, the failure of time–temperature superposition in disordered PIP–PVE diblocks is expected to be subtle compared to blends in which the component relaxations are well separated.

To interpret the BCP relaxation dynamics, it is desirable to draw upon the blend results, namely  $\zeta_{0,\text{PIP}}(\phi, T)$  and  $\zeta_{0,\text{PVE}}(\phi, T)$ . These also apply for the segments of each block of the present BCPs since (i) the BCPs are disordered, so the chain segments are in a homogenous, blend-like environment, and (ii) the blocks are long, so most of the segments are not influenced by either chain end or the block junction. Thus each block should have the same friction coefficient as the corresponding homopolymer chain in a blend with identical overall composition. The blend results suggest that failure of time–temperature superposition will be negligible for the high  $\phi_{\text{PIP}}$  BCP, where  $\zeta_{0,\text{PIP}} \approx \zeta_{0,\text{PVE}}$ , but noticeable for the low  $\phi_{\text{PIP}}$  BCP, where the disparity ( $\zeta_{0,\text{PIP}} < \zeta_{0,\text{PVE}}$ ) increases with decreasing temperature.

To infer the contribution of each block to the relaxation dynamics of the whole chain, we follow the method of Osaki<sup>17,18</sup> using the observed stress–optic behavior. In the next section we describe the polymers chosen as our model system and the rheo-optical instrument used. We then present the results of dynamic stress and birefringence measurements, comparing a diblock rich in the low  $T_g$  component ( $\phi_{\text{PIP}} = 0.75$ ) to one rich in the high  $T_g$  component ( $\phi_{\text{PIP}} = 0.25$ ). Next, the results are compared to the Doi–Edwards reptation model for mechanically uniform, entangled, linear polymers and to the dynamics of corresponding miscible blends.

## 2. Experimental Section

**2.1. Materials.** We choose as a model system diblock copolymers of 1,4-polyisoprene (PIP) and polyvinylethylene (PVE). The miscibility of PIP and PVE is well established;<sup>5,7,15,19</sup> hence these diblock copolymers remain in the disordered state under all experimental conditions. Furthermore, since the interactions are attractive,<sup>19</sup> fluctuation effects are suppressed. The synthesis and characterization of the diblock copolymers are described elsewhere.<sup>6</sup> To prevent oxidation, the polymers were stored under argon in a freezer ( $T \approx -10^\circ\text{C}$ ). The molecular weights of the diblock copolymers are sufficiently long that the shortest block is well entangled, with  $M > 11M_e$  (Table 1). The two pure species have very different mobilities at ambient temperatures, as a consequence

**Table 2. Stress–Optic Coefficients of Polyisoprene (PIP) and Polyvinylethylene (PVE) Homopolymers**

| $T$ (°C) | $C \times 10^{10}$ (cm <sup>2</sup> /dyne) |                    |
|----------|--|--------------------|
|          | PIP  | PVE                |
| 0        | 1.8 <sub>3</sub>                           | −0.3 <sub>0</sub>  |
| 10       | 1.7 <sub>8</sub>                           | −0.2 <sub>6</sub>  |
| 20       | 1.7 <sub>3</sub>                           | −0.2 <sub>3</sub>  |
| 30       | 1.6 <sub>9</sub>                           | −0.1 <sub>9</sub>  |
| 40       | 1.6 <sub>5</sub>                           | −0.1 <sub>6</sub>  |
| 50       | 1.6 <sub>1</sub>                           | −0.1 <sub>3</sub>  |
| 60       | 1.5 <sub>7</sub>                           | −0.1 <sub>1</sub>  |
| 80       | 1.5 <sub>1</sub>                           | −0.04 <sub>8</sub> |
| 110      | 1.4 <sub>2</sub>                           | +0.01 <sub>0</sub> |

of the large difference between their glass transition temperatures<sup>7,15,16</sup> ( $T_{g,\text{PIP}} \approx -60^\circ\text{C}$  and  $T_{g,\text{PVE}} \approx 0^\circ\text{C}$ ). To gain selective information regarding the relaxation of each block, we use the optical contrast inherent in this system.<sup>1</sup> The component stress–optic coefficients are of opposite signs and differ by an order of magnitude (Table 2).

**2.2. Rheo-optical Technique.** Dynamic mechanical and birefringence measurements are made using a rheo-optical instrument.<sup>20,21</sup> The strain, shear stress, birefringence, and its orientation are simultaneously recorded. Optical measurements are performed with the beam propagating along the vorticity axis (direction 3), measuring the birefringence in the plane given by the velocity (direction 1) and the velocity gradient (direction 2).

In small amplitude oscillatory shear  $\gamma(t) = \gamma_o \sin \omega t$ , the responses of the shear stress,  $\sigma_{12}$ , and the corresponding component of the refractive index tensor,  $n_{12}$ , are described by

$$\sigma_{12} = \gamma_o [G'(\omega) \sin \omega t + G''(\omega) \cos \omega t] \quad (1)$$

where  $G'(\omega)$  and  $G''(\omega)$  are the storage and loss moduli, and

$$n_{12} = \gamma_o [B'(\omega) \sin \omega t + B''(\omega) \cos \omega t] \quad (2)$$

where  $B'(\omega)$  and  $B''(\omega)$  are the components of the complex birefringence coefficient,  $B^*(\omega)$ .<sup>20,21</sup> To characterize departures from the stress–optic rule, we define the amplitude-based stress–optic ratio (SOR) and the phase difference between  $\sigma_{12}$  and  $n_{12}$ :

$$\text{SOR} \equiv |B^*|/|G^*| \quad (3)$$

and

$$\delta_B - \delta_G \equiv \tan^{-1}(B''/B') - \tan^{-1}(G''/G') \quad (4)$$

For homopolymer melts these are both independent of frequency, with SOR being the stress–optic coefficient,  $C_b$ , of homopolymer  $i$ ,<sup>22</sup> and  $\delta_B - \delta_G = 0$ . For disordered diblock copolymers the stress–optic rule is expected to fail<sup>17,18</sup> since the stress and birefringence will be differently weighted averages of the orientation of the segments comprising each block (i.e., the second moment of their segmental orientation distributions). This is particularly true if the blocks have  $C_i$ 's of opposite sign or widely differing magnitude.

Frequencies from 0.01 to 100 rad/s were employed at temperatures from 0 to 110 °C. At high frequencies and low temperatures, oscillatory strains of 1% or less were applied. With decreasing frequency and increasing temperature, when the force signal decreased to the limit of the transducer, the strain was increased. At the highest temperatures (95 and 110 °C) and the lowest frequencies, strains of 50–100% were used. In all cases, it was verified that the viscoelastic response was in the linear regime. At the lowest and highest temperatures, a nitrogen atmosphere was used. Experiments were performed at subambient temperatures first, then at ambient, at elevated temperatures, and then again at ambient to check for any changes, especially in the low frequency regime that is most sensitive to changes in molecular weight distribution.

**Table 3. Shift Factors,  $a_T$ , of Homopolymers and Block Copolymers**

| $T$ (°C) | homopolymers |          | block copolymers<br>(PIP–PVE w/w %) |         |
|----------|--------------|----------|-------------------------------------|---------|
|          | PIP          | PVE      | 75–25                               | 25–75   |
| 0        | 16           | 14 000   | 30                                  | —       |
| 10       | 5.3          | 300      | 8.5                                 | 40      |
| 15       | 3.3          | 18       | 4.0                                 | 14      |
| 20       | 2.2          | 12       | 2.9                                 | 5       |
| 30       | 1            | 1        | 1                                   | 1       |
| 40       | 0.51         | 0.15     | 0.44                                | 0.25    |
| 50       | 0.29         | 0.033    | 0.21                                | 0.080   |
| 60       | 0.17         | 0.009 5  | 0.12                                | 0.030   |
| 70       | 0.11         | 0.003 5  | 0.065                               | 0.013   |
| 80       | 0.072        | 0.001 4  | 0.040                               | 0.006 2 |
| 95       | 0.043        | 0.000 45 | 0.022                               | 0.002 5 |
| 110      | 0.027        | 0.000 22 | 0.014                               | 0.001 2 |

No evidence of cross-linking or degradation was observed in the experiments reported here, further confirmed by GPC characterization after rheo-optical testing.

### 3. Results

**3.1. Dynamic Moduli.** The BCP dynamic moduli resemble those of entangled, nearly monodisperse homopolymer melts, showing only one loss peak (Figures 1a and 2a), in accord with previous results on entangled disordered diblock copolymers far from the ordering transition.<sup>3,23,24</sup> Master curves were obtained by shifting the data only along the frequency axis so as to superimpose the terminal behavior at low frequencies (horizontal shift factors,  $a_T$ , are presented in Table 3, along with those of the homopolymers). If time–temperature superposition fails for these BCPs, it does so quite subtly and is not observable within the sensitivity of the experiments.

These results reproduce the dynamic moduli previously reported on these systems by Roovers and Wang,<sup>6</sup> (The magnitude of the cross over in the dynamic moduli is consistently lower by  $\sim 27\%$  than the literature values, as well as those for the pure components.<sup>4,14,25,26</sup> While we have been unable to account for this deviation, all our data are self-consistent and our conclusions are not affected.)

**3.2. Dynamic Birefringence.** The dynamic birefringence was measured simultaneously with the dynamic moduli. The stress–optic data are shown using the same reduced frequency as the dynamic moduli (Figures 1a and 2a, and Table 3). Excellent superposition of  $B'$  and  $B''$  is achieved for the case of  $\phi_{\text{PIP}} = 0.75$  using the mechanical shift factors (Figure 1b,c). However, shifting the complex birefringence according to the mechanical shift factors does *not* lead to time–temperature superposition for the  $\phi_{\text{PIP}} = 0.25$  block copolymer (Figure 2b,c). In fact, no set of shift factors yields superposition. This reveals changes in the shape of the relaxation spectrum with temperature—as expected on the basis of failure of time–temperature superposition for blends rich in PVE.<sup>2</sup>

The SOR of both block copolymers show distinct frequency dependencies (Figure 3): the stress–optic rule fails quite dramatically. At high frequencies the SOR of the  $\phi_{\text{PIP}} = 0.75$  BCP reaches a plateau that is approximately the composition-weighted average of the homopolymer stress–optic coefficients (see Table 2), very similar to the behavior of blends of the corresponding homopolymers.<sup>1,2</sup> This high frequency plateau is also accessible at low temperatures for the  $\phi_{\text{PIP}} = 0.25$  BCP, but is complicated by proximity to the dynamic glass transition, which causes the SOR to decrease at

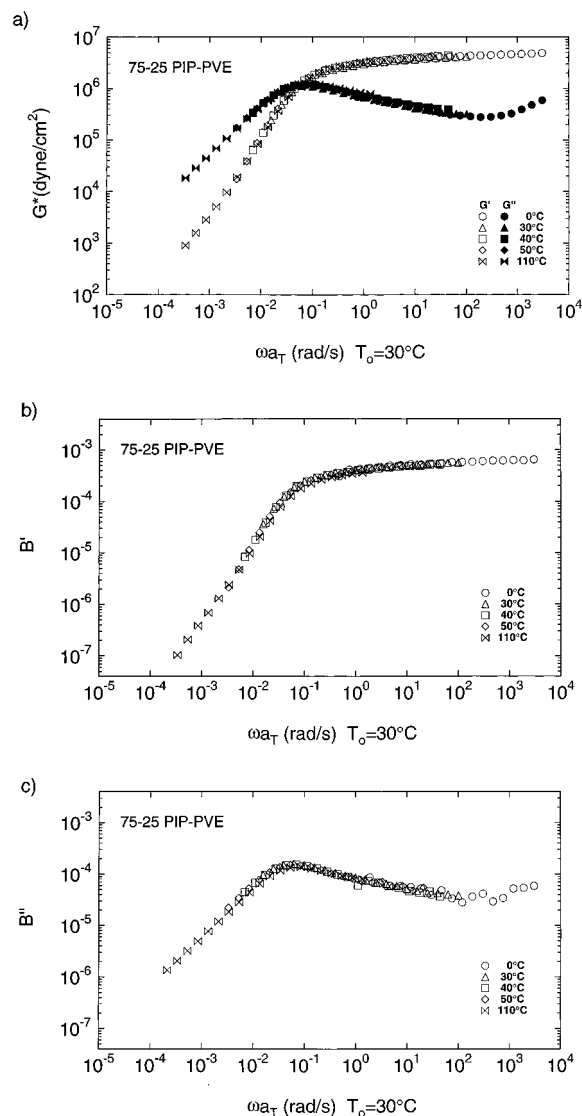


**Figure 1.** Dynamics of 75–25 PIP–PVE ( $\phi_{\text{PIP}} = 0.75$ ): Dynamic moduli, (a)  $G'$  and  $G''$ , and complex birefringence coefficients, (b)  $B'$  and (c)  $B''$ . The reference temperature is  $T_0 = 30^\circ\text{C}$ . Note that time–temperature superposition holds for  $G^*$  and  $B^*$ .

the highest reduced frequencies. With decreasing frequency the SOR rises when the shorter block has a negative stress–optic coefficient ( $\phi_{\text{PIP}} = 0.75$ , Figure 3a) and falls when the shorter block has a positive stress–optic coefficient ( $\phi_{\text{PIP}} = 0.25$ , Figure 3b). The characteristic reduced frequency of the upturn appears to be independent of temperature for the  $\phi_{\text{PIP}} = 0.75$  block copolymer (Figure 3a). However, for the block copolymer with  $\phi_{\text{PIP}} = 0.25$ , the characteristic frequency at which the SOR decreases shifts to lower reduced frequency as the temperature increases (Figure 3b). At low frequencies the BCP SOR reaches a second plateau whose value is closer to the stress–optic coefficient of the species which comprises the slowest relaxing section of the chain, i.e. the central portion.<sup>17,18,27–29</sup> The temperature dependence of the magnitude of SOR reflects that of the stress–optic coefficient for the dominant species, decreasing with temperature for the  $\phi_{\text{PIP}} = 0.75$  and increasing with temperature for the  $\phi_{\text{PIP}} = 0.25$  block copolymers.

The phase difference between the dynamic birefringence and shear stress,  $\delta_B - \delta_G$ , remains nearly zero for the  $\phi_{\text{PIP}} = 0.75$  BCP, with a slight dip (Figure 4) at

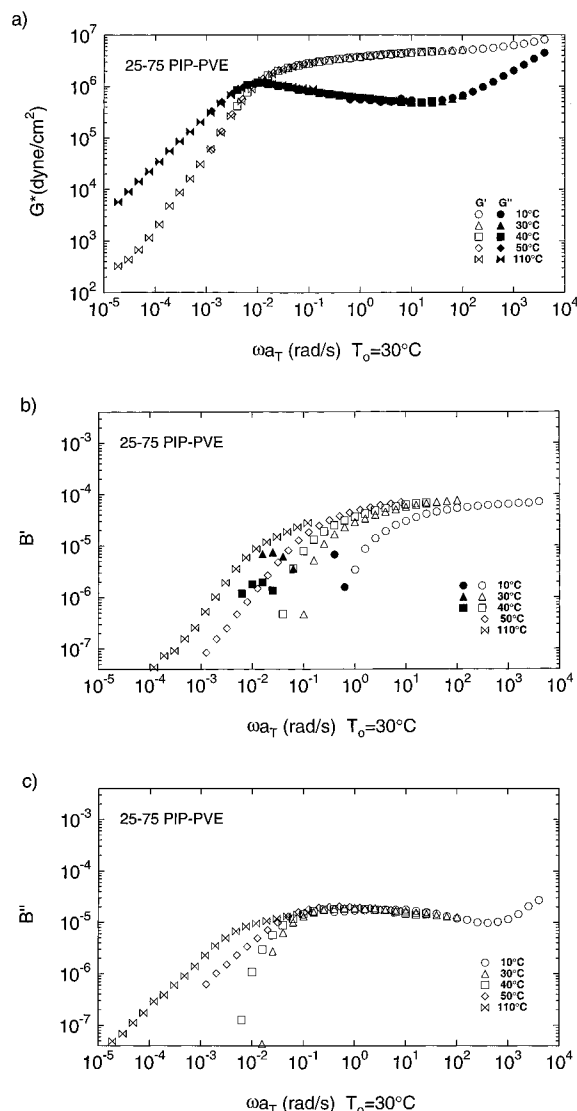


**Figure 2.** Dynamics of 25-75 PIP-PVE: Dynamic moduli, (a)  $G'$  and  $G''$ , and complex birefringence coefficients, (b)  $B'$  and (c)  $B''$ . The reference temperature is  $T_0 = 30^\circ\text{C}$ . Notice that while time-temperature superposition appears to hold on the basis of  $G^*$ , failure of time-temperature superposition is evident in  $B^*$ . Filled symbols in (b) correspond to values of  $B'$  which are negative.

the frequency of the upturn in SOR (Figure 3). Both the position and the depth of the minimum appear to be independent of temperature. The  $\phi_{\text{PIP}} = 0.25$  sample exhibits a dramatically different trend (Figure 4b). The phase difference has a large peak that changes shape and position with temperature. (The value of  $\delta_B - \delta_G$  even exceeds  $+\pi/2$  as the values of  $B'$  become negative; this is shown as a jump to  $-\pi/2$ , since the range is restricted to  $\pm\pi/2$ ).

#### 4. Discussion

Most of the salient features of the complex stress-optical behavior can be explained in terms of the relaxation of optically nonuniform chains, i.e. chains for which the segments of the two blocks have different anisotropic polarizabilities. Experimentally it has been observed that for a chain of uniform friction and entanglement molecular weight, the portions of the chain near the ends relax faster than the portions comprising the central part of the chain.<sup>17,18,27-29</sup>

For the  $\phi_{\text{PIP}} = 0.75$  block copolymer the upturn in SOR is indicative of the relaxation of the chain ends:

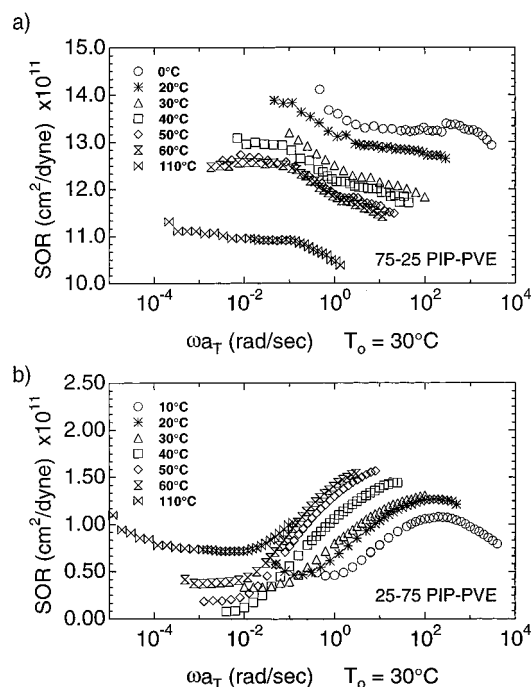


**Figure 3.** SOR of the block copolymers vs the same reduced frequencies as the dynamic moduli of the respective samples. The expanded vertical scale shows the inflection region of each SOR. Note that while for 75-25 PIP-PVE (a), the inflection remains at a fixed reduced frequency, that of 25-75 PIP-PVE (b) does not.

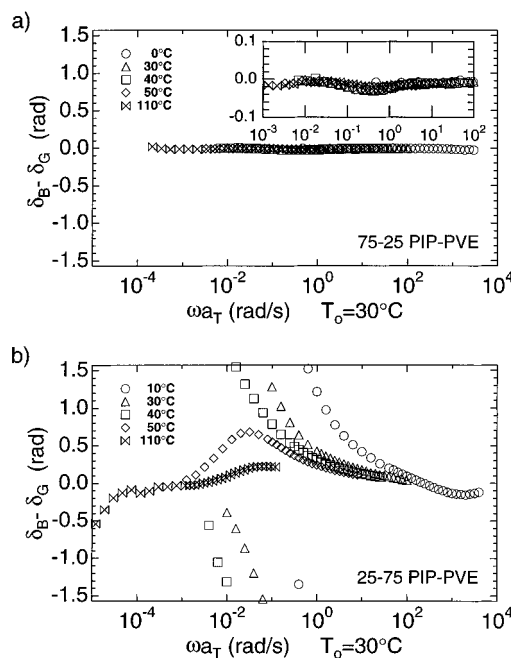


**Figure 4.** Phase difference between the dynamic birefringence and shear stress for the two BCP samples: (a) 75-25 PIP-PVE, (b) 25-75 PIP-PVE. The peak position for 25-75 PIP-PVE shifts to higher reduced frequency as the temperature increases.

as the negative contribution of the PVE block to the birefringence decays, the SOR increases toward that of PIP, which dominates the slower relaxing central portion of the chain. Conversely, for the  $\phi_{\text{PIP}} = 0.25$  BCP, relaxation of the ends reduces the positive contribution of the PIP block, which is manifested by a decrease in SOR with decreasing frequency as the chain center (PVE) contributes proportionally more to the SOR.

The temperature dependence of  $\text{SOR}(\omega a_T)$  is sensitive to departures from thermorheological simplicity. If the relaxation dynamics of the whole BCP chain shift the same way with temperature, then the horizontal shift factors determined from  $G^*(\omega)$  also superimpose  $B^*(\omega)$  and consequently  $\text{SOR}(\omega a_T)$ . While this may be the case for  $\phi_{\text{PIP}} = 0.75$  (Figure 3), it is definitely not the case for  $\phi_{\text{PIP}} = 0.25$ . In particular, the mechanical terminal relaxation speeds up more strongly with temperature than does the inflection in SOR; that is, the inflection in SOR moves to *lower* reduced frequency as the temperature increases. This relative shift indicates that the relaxation of the PIP end is less sensitive to temperature than that of the rest of the chain (PVE).

The relative phase of the birefringence and stress,  $\delta_B - \delta_G$ , shows corresponding signatures of the thermorheological simplicity of the  $\phi_{\text{PIP}} = 0.75$  BCP and the complexity of the  $\phi_{\text{PIP}} = 0.25$  BCP. For the  $\phi_{\text{PIP}} = 0.75$  BCP, the SOR is nearly constant and  $\delta_B \approx \delta_G$ , which is equivalent to the close resemblance between  $G'$  and  $B'$ , and  $G''$  and  $B''$  (Figure 1).

The dip in  $\delta_B - \delta_G$  corresponds to the relaxation of the PVE segments.<sup>1</sup> Since there is not a significant change in the relative relaxation rates between the two blocks with temperature,<sup>2</sup> the position of the dip in  $\delta_B - \delta_G$  remains at fixed reduced frequency and has approximately constant depth.

For the  $\phi_{\text{PIP}} = 0.25$  diblock, the relative phase shows significantly different behavior. As frequency decreases from the regime where the relative phase difference is approximately zero,  $\delta_B - \delta_G$  increases to large positive values, passing through  $+\pi/2$  to  $-\pi/2$  near where  $B'$  becomes negative (Figure 2). As the PIP end segments relax, the relative contribution of PVE to the in-phase stress and birefringence response increases, resulting in the decrease in  $B'$  and, at lower frequency,  $B''$ . In the terminal regime, where the central segments of PVE dominate the stress-optic response, the value of  $\delta_B - \delta_G$  returns to  $\sim 0$ . With increasing temperature the excursions of  $\delta_B - \delta_G$  from zero decrease since the value of the  $C_{\text{PVE}}$  becomes less negative relative to that of  $C_{\text{PIP}}$ . The frequency range where  $\delta_B - \delta_G$  deviates from zero shifts with temperature in the same way as the inflection in SOR. The movement of the inflection to lower frequency indicates a *decrease* in the relative rate of relaxation of the PIP block compared to the middle of the chain.

The behavior of the  $\phi_{\text{PIP}} = 0.75$  BCP suggests that it could be represented as an entangled chain that is mechanically uniform, but optically nonuniform (i.e., the blocks have approximately the same friction coefficient, but distinct stress-optic coefficients). The following section shows that this is the case by comparing the experimental results to the reptation model,<sup>27,30</sup> using the known temperature dependence of the stress-optic coefficients of PIP and PVE. The condition of mechanical uniformity is a reasonable approximation for the  $\phi_{\text{PIP}} = 0.75$  case, where results on PIP/PVE blends<sup>1,2,4,10,11</sup> show  $\zeta_{0,\text{PVE}}/\zeta_{0,\text{PIP}}$  only changes from 1.4 to 3.7 over the present temperature range. However, the restriction of the reptation model to mechanically uniform chains proves inadequate for the  $\phi_{\text{PIP}} = 0.25$  case, where  $\zeta_{0,\text{PVE}}/\zeta_{0,\text{PIP}}$  ranges from 1.4 to 15 over the same temperature range.

**4.1. Comparison to Reptation Model Predictions.** The stress-optical predictions of the reptation model are given by<sup>17,18,31</sup>

$$G'(\omega) = \sum_{\text{odd } p=1}^{\infty} \frac{1}{p^2} \frac{\omega^2 \tau_p^2}{1 + \omega^2 \tau_p^2}$$

$$G''(\omega) = \sum_{\text{odd } p=1}^{\infty} \frac{1}{p^2} \frac{\omega \tau_p}{1 + \omega^2 \tau_p^2} \quad (5)$$

$$B'(\omega) = \sum_{\text{odd } p=1}^{\infty} C_p \frac{1}{p^2} \frac{\omega^2 \tau_p^2}{1 + \omega^2 \tau_p^2}$$

$$B''(\omega) = \sum_{\text{odd } p=1}^{\infty} C_p \frac{1}{p^2} \frac{\omega \tau_p}{1 + \omega^2 \tau_p^2} \quad (6)$$

The optical weighting factors,  $C_p$  are

$$C_p = 1/2 \{ (q_A + q_B) + (q_B - q_A) \cos(\pi p f_A) \} \quad (7)$$

where  $q_i$  are the species' anisotropic polarizabilities (proportional to their stress-optic coefficients),  $p$  is the mode number ( $p = 1$  corresponds to the longest relaxation time of the chain, the disengagement time,  $\tau_d$ ; the higher modes have  $\tau_p = \tau_d/p^2$ ) and  $f_A$  is the fractional length of block A.<sup>31</sup> Equations for SOR and  $\delta_B - \delta_G$  are given in the Experimental Section.

The qualitative features of the observed SOR and  $\delta_B - \delta_G$  are captured by the dynamics of a reptating, mechanically uniform diblock ( $\zeta_{0,A} = \zeta_{0,B}$  and  $M_{e,A} = M_{e,B}$ ) in which the two blocks have different stress-optic coefficients. The assumption of uniform entanglement molecular weights of the two blocks is a good approximation for the PIP/PVE system.<sup>4,25,26</sup> The relative block lengths in the model are set to correspond to those of the two diblock copolymers, measured in units of their respective entanglement molecular weights. We take the terminal relaxation time,  $\tau_d$ , of each chain to equal  $2/\omega_x$  where  $\omega_x$  is the cross-over frequency of the dynamic moduli (Figures 1a and 2a).<sup>1</sup>

The optical properties,  $q_i$ , of each block are set to correspond to the homopolymer values of  $C_{\text{PIP}}(T)$  and  $C_{\text{PVE}}(T)$  (Table 2). In the absence of internal field effects or changes in local chain configuration upon blending, each segment in the BCP contributes to the birefringence in proportion to its contribution to the stress, with the constant of proportionality being the stress-optic coefficient  $C_i$  of the pure species  $i$ .<sup>1</sup>

The linear dependence of the high-frequency plateau in SOR with composition suggests this is a good approximation for PIP/PVE.<sup>1,2</sup> This is to be expected since changes in local chain statistics due to blending are negligible in PIP/PVE blends.<sup>7,15,19</sup> The consequences of connectivity of the two blocks on the segmental distribution should also be negligible except for the small fraction of segments near the junction, since each block is long.

We first consider a model that neglects orientational coupling. The reptation model (Figure 5) captures the inflection observed in the experimental SOR (Figure 3). The temperature dependencies of  $C_{\text{PIP}}(T)$  and  $C_{\text{PVE}}(T)$  are primarily responsible for the vertical shift of the observed SOR with temperature. The model correctly predicts the general *shapes* of the relative phase differences,  $\delta_B - \delta_G$  for both BCPs (Figure 6). Experimentally, the reduced frequency at which the upward inflection occurs in SOR and the dip occurs in  $\delta_B - \delta_G$  for the  $\phi_{\text{PIP}} = 0.75$  diblock does not change with temperature (Figures 3a and 4a), in accord with the

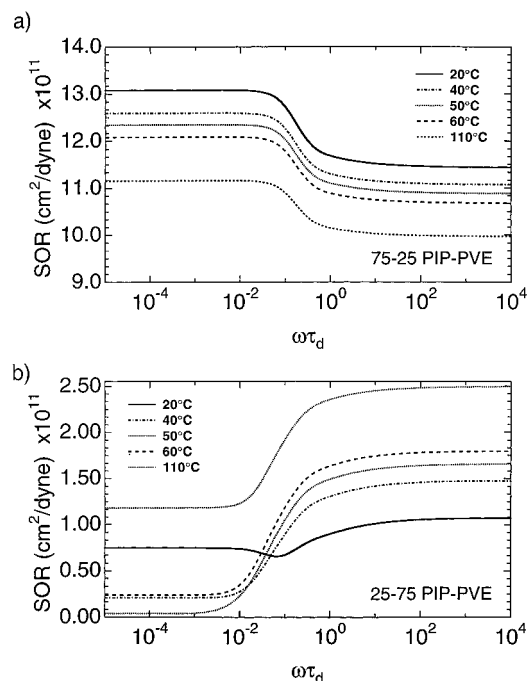


**Figure 5.** Calculated BCP SOR based on the reptation model, under the assumption of chains of uniform friction coefficient and statistical segment length (mechanical uniformity). The stress-optic coefficients of the homopolymer species at each temperature are used to determine the optical properties of the chain at the temperatures indicated in the legend. See the text for discussion.

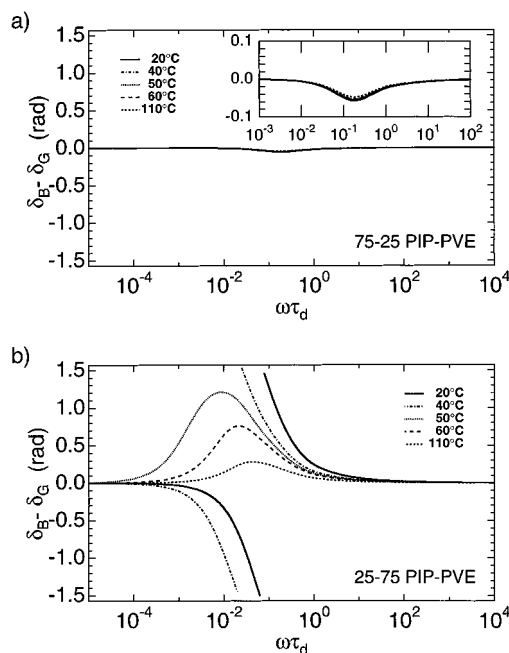


**Figure 6.** Calculated phase difference between dynamic birefringence and stress for a mechanically uniform reptation model. See the text for discussion.

model. In contrast, the experimental data show that the inflection in SOR for the  $\phi_{PIP} = 0.25$  diblock moves to lower reduced frequency as temperature increases (Figure 3b). This is in disagreement with the mechanically uniform reptation model. In addition, for the  $\phi_{PIP} = 0.25$  BCP the magnitude and frequency dependence of  $\delta_B - \delta_G$  is in disagreement with experiment. These discrepancies persist even when the effects of orientational coupling<sup>31,32</sup> are included, using the values of the coupling coefficient determined previously for the PIP/

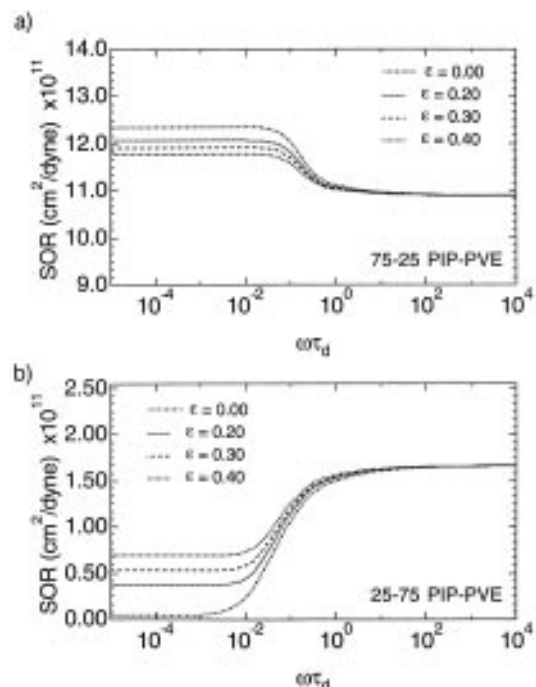


**Figure 7.** Calculated BCP SOR based on the mechanically uniform reptation model at 50 °C. The coupling coefficient,  $\epsilon$ , is varied from 0 to 0.40. Results at other temperatures show similar behavior.

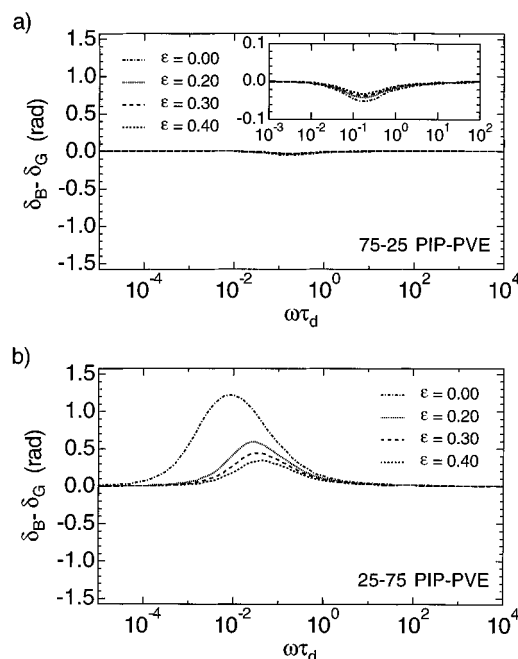


**Figure 8.** Calculated phase difference between dynamic birefringence and shear stress for a mechanically uniform reptation model at 50 °C. The coupling coefficient,  $\epsilon$ , is varied from 0 to 0.40. Results at other temperatures show similar behavior.

PVE system.<sup>2,10,11</sup> Orientational coupling merely reduces the magnitude of the departure from the stress-optic rule (smaller step in SOR and smaller peak/valley in  $\delta_B - \delta_G$ ); it does not shift the frequency dependence of SOR (Figure 7).

The success of the model in reproducing the essential features observed experimentally for the  $\phi_{PIP} = 0.75$  BCP is in accord with the established dynamics of PIP/PVE blends rich in PIP, in which both PIP and PVE shift nearly the same way with temperature ( $1.4 \leq$

**Table 4. Friction Coefficients of Polyisoprene and Polyvinylethylene in Blends**

| $T$ (°C) | $\phi_{\text{PIP}} = 0.75$   |                              | $\phi_{\text{PIP}} = 0.25$   |                              |
|----------|------------------------------|------------------------------|------------------------------|------------------------------|
|          | $\zeta_{0,\text{PIP}}$ (g/s) | $\zeta_{0,\text{PVE}}$ (g/s) | $\zeta_{0,\text{PIP}}$ (g/s) | $\zeta_{0,\text{PVE}}$ (g/s) |
| -10      | $6.5 \times 10^{-5}$         | $2.4 \times 10^{-4}$         | —                            | —                            |
| 5        | $7.9 \times 10^{-6}$         | $2.5 \times 10^{-5}$         | $1.8 \times 10^{-4}$         | $2.7 \times 10^{-3}$         |
| 15       | $2.4 \times 10^{-6}$         | $4.7 \times 10^{-6}$         | $2.5 \times 10^{-5}$         | $2.7 \times 10^{-4}$         |
| 25       | $8.9 \times 10^{-7}$         | $3.1 \times 10^{-6}$         | $5.3 \times 10^{-6}$         | $4.1 \times 10^{-5}$         |
| 40       | $3.2 \times 10^{-7}$         | $7.4 \times 10^{-7}$         | $1.0 \times 10^{-6}$         | $5.0 \times 10^{-6}$         |
| 60       | $1.0 \times 10^{-7}$         | $1.6 \times 10^{-7}$         | $2.1 \times 10^{-7}$         | $6.1 \times 10^{-7}$         |
| 80       | $4.1 \times 10^{-8}$         | $5.5 \times 10^{-8}$         | $6.7 \times 10^{-8}$         | $1.2 \times 10^{-7}$         |
| 110      | $1.7 \times 10^{-8}$         | $2.4 \times 10^{-8}$         | $1.9 \times 10^{-8}$         | $2.7 \times 10^{-8}$         |

$[\zeta_{0,\text{PVE}}/\zeta_{0,\text{PIP}}] \leq 3.7$  for  $110^\circ\text{C} \leq T \leq -10^\circ\text{C}$ ). For the  $\phi_{\text{PIP}} = 0.75$  BCP, the mechanically uniform reptation model is a good approximation and successfully reproduces the reduced frequency and temperature dependence of the stress-optic data (Figure 5).

The failure of the model in capturing the behavior of the  $\phi_{\text{PIP}} = 0.25$  BCP is in qualitative accord with the appearance of thermorheological complexity in blends rich in PVE. Previous work on PIP/PVE blends has shown that the failure of time-temperature superposition observed for this system can be attributed to the distinct temperature dependence of each species' dynamics in the blend.<sup>1,2,4,10-13</sup> For the  $\phi_{\text{PIP}} = 0.25$  BCP, the shift of the inflection in SOR with temperature can be understood in terms of the relative rates of relaxation of the two blocks. Since the shift factor is based on the slowest relaxation modes, the reduced frequency scale is appropriate for the center of the chain, which consists of PVE in this diblock. This is consistent with the established temperature dependence of the friction coefficients of PIP and PVE in a  $\phi_{\text{PIP}} = 0.25$  environment (Table 4). The relative rate of relaxation of the PIP block decreases because the contrast in monomeric friction is large at low temperature ( $\zeta_{0,\text{PVE}}/\zeta_{0,\text{PIP}} = 15$  at  $5^\circ\text{C}$ ), and decreases significantly with increasing temperature ( $\zeta_{0,\text{PVE}}/\zeta_{0,\text{PIP}} = 1.4$  at  $110^\circ\text{C}$ ).

The reptation model also fails to capture the magnitude of the relative phase difference,  $\delta_B - \delta_G$ . This is not due to any scaling prefactors neglected in the calculation of the dynamic moduli or birefringence coefficients, since only ratios of these quantities determine the relative phase difference. Such disagreement is a consequence of the assumption of uniform friction along the chain.

## 5. Conclusions

Coordinated analysis of the shear stress and birefringence in dynamic shear is used to monitor the relaxation of each block in a disordered diblock copolymer. Qualitatively, the frequency dependence of the complex stress-optic behavior can be explained in terms of the relaxation of chains with blocks having distinct stress-optical coefficients, with the center portion of the BCP dominating at low frequencies. Quantitatively, comparison to predictions of the reptation model reveals that a diblock in which the friction coefficients of the distinct blocks are similar relaxes like a chain having uniform friction, as is the case for the  $\phi_{\text{PIP}} = 0.75$  diblock. On the other hand, if there is significant contrast between the friction coefficients of the two blocks, combined with a change in this contrast with temperature, then departure from the uniform-friction relaxation dynamics can be significant. This is observed when the diblock is rich in PVE.

Failure of time-temperature superposition for the mechanical moduli is not noticeable for these BCPs

because the relaxation spectrum is always nearly that of a monodisperse homopolymer. However, the lack of superposition of SOR using the mechanically determined shift factors shows that failure of time-temperature superposition is in fact present. These results eliminate the paradox raised by the apparent disappearance of thermorheological complexity in miscible block copolymers, even in systems that show complexity in the corresponding miscible blends. Stress-optical behavior provides a more sensitive signature of the relaxation dynamics and shows that time-temperature superposition does fail for both BCPs and blends when the composition is rich in the high  $T_g$  species.

**Acknowledgment.** We gratefully acknowledge the support of the National Science Foundation Presidential Young Investigator Award (J.A.K.), the National Physical Science Consortium (B.H.A.), the Caltech Summer Undergraduate Research Fellowship Program (K.S.), Chevron, and the Caltech Consortium in Chemistry and Chemical Engineering: E. I. du Pont de Nemours and Company, Inc. and Eastman Kodak Company. We thank Dr. Fei Wang for preparing and characterizing the polymers.

## References and Notes

- (1) Arendt, B. H.; Kannan, R. M.; Zewail, M.; Kornfield, J. A.; Smith, S. *Rheol. Acta* **1994**, *33*, 322. Arendt, B. H. *et al. Proceedings of the ACS, PMSE, Washington, DC*, **1994**, 71, 471.
- (2) Arendt, B. H.; Krishnamoorti, R.; Kornfield, J. A.; Smith, S. D. *Macromolecules* **1997**, *30*, 1127 (preceding manuscript in this journal).
- (3) Bates, F. S.; Rosedale, J. H.; Fredrickson, G. H. *J. Chem. Phys.* **1990**, *92*, 6255.
- (4) Roovers, J.; Toporowski, P. M. *Macromolecules* **1992**, *25*, 3454.
- (5) Bates, F. S.; Rosedale, J. H.; Bair, H. E.; Fredrickson, G. H. *Macromolecules* **1989**, *21*, 2557.
- (6) Roovers, J.; Wang, F. *J. Non-Cryst. Solids*, **1994**, 172-4, 698.
- (7) Trask, C. A.; Roland, C. M. *Macromolecules* **1989**, *22*, 256.
- (8) Kanetakis, J.; Fytas, G.; Kremer, F.; Pakula, T. *Macromolecules* **1992**, *25*, 3484. Fytas, G.; Meier, G.; Richter, D. *J. Chem. Phys.* **1996**, *105*, 1208.
- (9) Alegria, A.; Colmenero, J.; Ngai, K. L.; Roland, C. M. *Macromolecules* **1994**, *27*, 4486.
- (10) Zawada, J. A.; Fuller, G. G.; Colby, R. H.; Fetters, L. J.; Roovers, J. *Macromolecules* **1994**, *27*, 6851.
- (11) Zawada, J. A.; Fuller, G. G.; Colby, R. H.; Fetters, L. J.; Roovers, J. *Macromolecules* **1994**, *27*, 6861.
- (12) Chung, G. C.; Kornfield, J. A.; Smith, S. D. *Macromolecules* **1994**, *27*, 964.
- (13) Chung, G. C.; Kornfield, J. A.; Smith, S. D. *Macromolecules* **1994**, *27*, 5729.
- (14) Roovers, J.; Toporowski, P. M. *Rubber Chem. Tech* **1990**, *63*, 734.
- (15) Roland, C. M. *Macromolecules* **1987**, *20*, 2557.
- (16) Roland, C. M. *J. Polym. Sci., Polym. Phys. Ed.* **1988**, *26*, 839.
- (17) Osaki, K.; Takatori, E.; Kurata, M.; Ohnuma, H.; Kotaka, T. *Polymer* **1986**, *18*, 947.
- (18) Osaki, K.; Takatori, E.; Ueda, M.; Kurata, M.; Kotaka, T.; Ohnuma, H. *Macromolecules* **1989**, *22*, 2457.
- (19) Tomlin, D. W.; Roland, C. M. *Macromolecules* **1992**, *25*, 2994.
- (20) Kannan, R. M.; Kornfield, J. A. *Macromolecules* **1994**, *27*, 1177.
- (21) Kannan, R. M.; Kornfield, J. A. *J. Rheol.* **1994**, *38*, 1127.
- (22) Janeschitz-Kriegl, H. *Polymer Melt Rheology and Flow Birefringence*; Springer-Verlag: Berlin, 1983.
- (23) Kim, J. K.; Han, C. D. *Macromolecules* **1992**, *25*, 271.
- (24) Rosedale, J. H.; Bates, F. S. *Macromolecules* **1990**, *23*, 2329.
- (25) Carella, J. M.; Graessley, W. W.; Fetters, L. J. *Macromolecules* **1984**, *17*, 2775.
- (26) Gotro, J. T.; Graessley, W. W. *Macromolecules* **1984**, *17*, 2767.
- (27) Doi, M.; Edwards, S. F. *The Theory of Polymer Dynamics*; Oxford University Press: Oxford, 1986.

- (28) Tassin, J. F.; Monnerie, L.; Fetters, L. J. *Macromolecules* **1988**, *21*, 2404.
- (29) Ylitalo, C. M.; Fuller, G. G.; Abetz, V.; Stadler, R.; Pearson, D. S. *Rheol. Acta* **1990**, *29*, 543.
- (30) deGennes, P. G. *J. Chem. Phys.* **1971**, *55*, 572.
- (31) Lodge, T. P.; Amelar-Lodge, S. *Rheol. Acta* **1992**, *31*, 32.
- (32) Doi, M.; Pearson, D. S.; Kornfield, J. A.; Fuller, G. G. *Macromolecules* **1989**, *22*, 1488.
- (33) Ferry, J. D. *Viscoelastic Properties of Polymers*; Wiley: New York, 1980.
- (34) Larson, R. G. *Constitutive Equations for Polymer Melts and Solutions*; Butterworths: Boston, 1988.
- (35) Man, V. F.; Schrag, J. L.; Lodge, T. P. *Macromolecules* **1991**, *24*, 3666.
- (36) Rouse, P. E. *J. Chem. Phys.* **1953**, *21*, 1272.
- (37) Wang, F. W. *Macromolecules* **1975**, *8*, 364.
- (38) Wang, F. W. *Macromolecules* **1998**, *11*, 1198.

MA960902D